PAPER

The computation of local stress in *ab initio* molecular simulations

IOP Publishing Modelling and Simulation in Materials Science and Engineering
Modelling Simul. Mater. Sci. Eng. **27** (2019) 065016 (16pp) https://doi.org/10.1088/1361-651X/ab2b8a

The computation of local stress in *ab initio* molecular simulations

Xiantao Li

Department of Mathematics, The Pennsylvania State University, University Park, PA 16802, United States of America

E-mail: xxl12@psu.edu

Received 14 December 2018, revised 13 June 2019
Accepted for publication 20 June 2019
Published 2 July 2019

Abstract

Motivated by the increasingly more important role of *ab initio* molecular dynamics models in material simulations, this work focuses on the definition of local stress, when the forces are determined from quantum-mechanical (QM) descriptions. Two types of *ab initio* models, including the Born–Oppenheimer and Ehrenfest dynamics, are considered. In addition, formulas are derived for both tight-binding and real-space methods for the approximations of the QM models. The formulas are examined via comparisons with full *ab initio* molecular simulations.

Keywords: *ab initio* molecular dynamics, Irvine–Kirkwood formalism, density-functional theory

(Some figures may appear in colour only in the online journal)

1. Introduction

The last few decades have witnessed considerable interest in *ab initio* molecular dynamics (AIMD) as a simulation tool in chemistry and material science [1–3]. Compared to classical molecular dynamics (MD), where the interatomic potential is constructed in advance, AIMD determines on-the-fly the forces on the ions from quantum-mechanical (QM) degrees of freedom, which remain active throughout the computation. AIMD is particularly suitable for problems where classical MD models are difficult to construct, e.g. alloys with multiple species and material interfaces, and problems where there are significant changes in the chemical environment, e.g. bonding patterns. There have been great recent progress in the development of efficient AIMD models, see the reviews [1, 4] for more details. Various software packages have also been developed and widely used [5–7].

Due to the advent of growing computing powers, it is conceivable that AIMD will soon be applied to large-scale mechanical systems, at which point, studying the elastic field

induced by lattice defects, boundary conditions, electric fields, etc would be of interest. It would then be of great practical importance to derive the atomic-level stress from AIMD. This was already noted in the pioneering work of Nielsen and Martin [8, 9], where the notion of *total* stress has been established by applying a uniform strain and taking the variation of the total energy with respect to the strain tensor. This approach was later extended by Filippetti and Fiorentini [10], who continued this path and introduced the stress density, whose integral recovers the total stress. Numerical implementations have been proposed by Shiihara *et al* [11, 12], where they still considered a uniform strain applied to the system. Vitek and Egami [13] emphasized the fact that the local stress can be generated by local disorder. Based on the work of Nielsen and Martin, the local stress, called the atomic level stress, was identified around each atom site. A more general approach is proposed by Rogers and Rappe [14], where local stress is defined using a non-homogeneous strain by the principle of virtual work.

Meanwhile, for classical MD models, there have been consistent mathematical frameworks for the definition and computational methods for the *local* stress, mostly motivated by the Irving–Kirkwood formalism [15], which starts with the Liouville equation for the many-particle density, and hydrodynamics equations can be obtained by taking the ensemble average with respect to the distribution function. In principle, this formalism is applicable to systems that are in or out of equilibrium. In practice, a more popular approach is the Hardy's formulation [16, 17], which starts directly with the local density and momentum distributions. Following the Newton's equations of motion in the MD model, fundamental conservation laws can be derived, and the local stress can be identified from the momentum balance. Effectively, this amounts to replacing the delta functions in the Irving-Kirkwood formalism by certain smooth kernel functions. There has been tremendous recent progress toward the definition and computation of such local stress, see [18–39] and the references therein for recent development.

The primary goal of this paper is to establish the notion of local stress in AIMD models. The notion of local stress has been presented by Nielsen and Martin [40] in the context of many-particle QM models. It is also derived using the momentum balance equation. In the practical case where the electron structures are described by the density-functional theory (DFT) [41], however, only the *total* stress was presented in [40]. We will present in this paper the derivation of the local stress for models based on DFT and its extensions [42, 43]. Our approach is motivated by the success in the classical MD models, and the main ingredient is the momentum balance and a consistent decomposition of the atomic forces. Due to the wide variety of AIMD models, we will focus on two widely implemented models, including the Born–Oppenheimer MD (BOMD) and the Ehrenfest dynamics. The BOMD approach involves solving the time-independent eigenvalue problem at each time step, while in Ehrenfest dynamics, the wave functions are determined by solving the time-dependent Schrödinger equation (TDSE) in real time, e.g. to study the response of graphene to external electric field [44]. In both cases, the formulas for computing the total force on an ion are similar.

Of particular importance for the definition of the local stress is the distribution of the force among each pair of ions, as extensively studied in classical MD [18, 21, 22, 33, 36–39]. We show that the force decomposition critically depends on how the QM models are discretized in space. We discuss two specific implementations, the tight-binding (TB) approach, where the wave functions are approximated by linear combinations of atomic orbitals, and the real-space approximations, e.g. finite-difference or finite element approximations. In the former approach, the basis functions are centered around ion positions, while in the latter

approach, the grid points remain fixed in the computation. We will show that the force decomposition is rather straightforward in the former approach, since the interatomic distance is naturally involved in the Hamiltonian matrix. However, for real space methods, since the grid points are not attached to ion positions, such force decomposition is rather non-trivial.

The rest of the paper is organized as follows. In section 2, we review the AIMD models, as well as the definition of stress in classical MD models. The TB approximation, along with the stress definition, will be presented in section 3. In section 4, we discuss the real-space approximation methods, and we present some numerical results.

2. *Ab initio* molecular models and fundamental conservation laws

Throughout the paper, we will denote the ion positions by R_I, and the coordinate for the electronic wave functions by $\boldsymbol{r}$. The elastic field will be defined in terms of the spatial variable $\boldsymbol{x}$. We assume that the system under consideration consists of N_{ion} ions, and N_{ele} electrons.

2.1. Two AIMD models

Let us start with the Newton's equations of motion for the ions

$$\begin{cases} \dot{R}_I &= P_I/m_I, \\ \dot{P}_I &= -\dfrac{\partial}{\partial R_I} E_{\text{tot}}, \quad I = 1, 2, \cdots, N_{\text{ion}}. \end{cases} \tag{1}$$

Here m_I is the mass; R_I and $_{PI}$ represent the coordinate and momentum of the nuclei, respectively. The main departure of AIMD from conventional MD models is that the potential energy E_{tot} is determined from an underlying QM description, instead of using a pre-determined interatomic potential. How the electronic degrees of freedom are introduced, on the other hand, leads to different formulations of AIMD. We will consider two models that have been widely implemented. Extensions to other models, e.g. [3, 45–49], especially the Car–Perrinello approach [3], are likely to be straightforward.

BOMD. First, we consider the BOMD model, where at each step, one solves a time-independent eigenvalue problem

$$\hat{H}\psi_\ell = \varepsilon_\ell \psi_\ell, \quad \ell = 1, 2, \cdots, N_{\text{ele}}. \tag{2}$$

Again we denote the number of electrons by N_{ele}.

For the Hamiltonian operator $\hat{H}$, we will consider the DFT [41], which uses a non-interacting system with an exchange-correlation function that reproduces the ground-state electronic density of the full, interacting system. The Hamiltonian operator $\hat{H}$ (in reduced units) consists of the kinetic energy, Hartree and exchange correlation, and the external potential

$$\hat{H} = -\frac{\nabla^2}{2} + \hat{V}_H[n] + \hat{V}_{\text{xc}}[n] + \hat{V}_{\text{ext}}. \tag{3}$$

We will denote the second and third terms, which are functionals of the electron density, as Kohn–Sham potential

$$\hat{V}_{\text{KS}} = \hat{V}_H[n] + \hat{V}_{\text{xc}}[n], \tag{4}$$

where

$$n(\boldsymbol{r},\, t) = \sum_{\ell=1}^{N_{\text{ele}}} n_\ell |\psi_\ell(\boldsymbol{r},\, t)|^2, \tag{5}$$

is the total electron density. The coefficients n_ℓ are the occupation numbers.

The Hamiltonian operator $\hat{H}$ depends on the ion's positions, which contribute to the electronic structure as an external potential $\hat{V}_{\text{ext}}$. This will be explained in more details in the next section. As a result, the eigenvalue problems need to be solved repeatedly, since the position of the ions is changing continuously. After each eigenvalue problem is solved, the total energy and force on each atom are computed as follows

$$E_{\text{tot}} = \sum_{\ell=1}^{N_{\text{ele}}} n_\ell \varepsilon_\ell, \quad \boldsymbol{f}_I = -\frac{\partial E_{\text{tot}}}{\partial R_I}, \quad I = 1,\, 2,\, \cdots,\, N_{\text{ion}}. \tag{6}$$

The coupled system (1) and (2) are the basis of BOMD models, which can be interpreted as differential-algebraic equations. The main assumptions is that the electronic states are instantaneously relaxed to ground states during the movement of the nuclei. Typically, the explicit formulas for computing the forces (6) are derived based on the Hellmann–Feymann theorem. We will discuss these formulas in the context of TB and real-space approximations.

Ehrenfest dynamics. Another type of AIMD models is the Ehrenfest dynamics, e.g. [48], where wave functions are determined from the TDSEs

$$\mathrm{i}\partial_t \psi_\ell = \hat{H}\psi_\ell, \tag{7}$$

in conjunction with the Newton's equations of motion for the ions (1). The coupled dynamics describes an ion–electron coupling that occurs continuously in time. For the time-dependent model, we consider the time-dependent density-functional theory (TDDFT), and the model has been widely used to compute the excitation states and responses to electric and magnetic fields [42, 43, 50].

In this case, the formula for computing the forces in (6) will be the same as in the static case, but for the reason that the wave functions and ion positions are independent variables.

2.2. The definition of local stress based on momentum balance and force decomposition

Since the Newton's equations (1) remain the same in all AIMD models, the fundamental conservation law of momentum still holds. More specifically, given the momenta and coordinates of the nuclei, we define the local momentum

$$\boldsymbol{j}(\boldsymbol{x},\, t) = \sum_{I=1}^{N_{\text{ion}}} P_I(t)\varphi(\boldsymbol{x} - R_I(t)). \tag{8}$$

This is the starting point in Hardy's derivation of stress [16], which we will follow here. The function φ is introduced as an approximation to the Dirac delta function in the original Irving–Kirkwood formalism [15], and it is assumed to be non-negative with integral being 1. More specifically, by taking time derivative, one gets

$$\begin{aligned}\partial_t \boldsymbol{j} = &-\nabla_{\boldsymbol{x}} \cdot \left[\sum_{I=1}^{N_{\text{ion}}} P_I(t) \otimes P_I(t)\varphi(\boldsymbol{x} - R_I(t))\right] \\ &+ \sum_{I=1}^{N_{\text{ion}}} \boldsymbol{f}_I(t)\varphi(\boldsymbol{x} - R_I(t)).\end{aligned} \tag{9}$$

The conservation of momentum at the continuum level asserts that

$$\partial_t \boldsymbol{j} = \nabla_{\boldsymbol{x}} \cdot \boldsymbol{\sigma}, \tag{10}$$

with $\boldsymbol{\sigma}$ being the total stress tensor. So the goal is to express the right-hand side of the equation (9) as a divergence form.

This will be true if the force $\boldsymbol{f}_I$ exhibits the following patterns:

(i) the force can be decomposed among each pair of atoms (I, J):

$$\boldsymbol{f}_I = \sum_{J \neq I} \boldsymbol{f}_{IJ}, \tag{11}$$

(ii) each component is skew-symmetric

$$\boldsymbol{f}_{IJ} = -\boldsymbol{f}_{JI}, \tag{12}$$

(iii) $\boldsymbol{f}_{IJ}$ is local, it should decay quickly as a function of the interatomic distance.

The first two conditions are critical (and sufficient) to ensure the conservation of momentum. It is worthwhile to point out, although it is trivial to many, that the fact that the force can be decomposed as in (11) does not by any means imply that the interaction is pairwise. In fact, the force component $\boldsymbol{f}_{IJ}$ may depend on atoms other than the two atoms I and J. The last property is not mandatory. However, when the forces are highly non-local, the computation would be much more expensive, since many particles have to be visited.

To see why such force decomposition is necessary, we can substitute (11) into the second term on the right-hand side of (9), which yields

$$\begin{aligned}
\sum_{I=1}^{N_{\text{ion}}} \sum_{J=1}^{N_{\text{ion}}} \boldsymbol{f}_{IJ}\, \varphi(\boldsymbol{x} - R_I(t)), &= \frac{1}{2} \sum_{I=1}^{N_{\text{ion}}} \sum_{J=1}^{N_{\text{ion}}} [\boldsymbol{f}_{IJ}\, \varphi(\boldsymbol{x} - R_I(t)) + \boldsymbol{f}_{JI}\, \varphi(\boldsymbol{x} - R_J(t))] \\
&= \frac{1}{2} \sum_{I=1}^{N_{\text{ion}}} \sum_{J=1}^{N_{\text{ion}}} \boldsymbol{f}_{IJ} [\varphi(\boldsymbol{x} - R_I(t)) - \varphi(\boldsymbol{x} - R_J(t))] \\
&= -\nabla \cdot \frac{1}{2} \sum_{I=1}^{N_{\text{ion}}} \sum_{J=1}^{N_{\text{ion}}} \boldsymbol{f}_{IJ} \otimes R_{IJ} B_{IJ}.
\end{aligned}$$

Here in the last step, we used the fundamental theorem of calculus, and converted the difference between the two terms into a line integral along $R_{IJ} = R_I - R_J$,

$$B_{IJ}(\boldsymbol{x}) = \int_0^1 \varphi(\boldsymbol{x} - R_J - \lambda R_{IJ}) \mathrm{d}\lambda. \tag{13}$$

This derivation reveals a divergence term, from which one can identify the local stress

$$\boldsymbol{\sigma} = -\sum_{I=1}^{N_{\text{ion}}} P_I(t) \otimes P_I(t) \varphi(\boldsymbol{x} - R_I(t)) - \frac{1}{2} \sum_{I=1}^{N_{\text{ion}}} \sum_{J=1}^{N_{\text{ion}}} \boldsymbol{f}_{IJ} \otimes R_{IJ} B_{IJ}(\boldsymbol{x}). \tag{14}$$

It is clear that such definition is always up to a divergence-free term, which makes it non-unique. This is a common observation [18]. One interpretation is to integrate the momentum balance equation (9) over an arbitrary domain. Using the divergence theorem, one would obtain the traction along the boundary, in the form of a pairwise force $\boldsymbol{f}_{IJ}$, which is consistent with Cauchy's notion of stress. The momentum in the first term can be further decomposed into a mean $(\boldsymbol{j}(\boldsymbol{x}, t))$ and a relative momentum. They lead to the convection term, which typically appears on the left-hand side of the momentum balance equation, and a kinetic stress term, e.g. see the derivations in [30]. But our focus will be on the potential part of the stress

(the last term). The line integral along each pair of atoms comes out naturally in the Irving–Kirkwood and Hardy's formulation. But it did not arise from the derivation of the stress density from QM descriptions [8–12].

In the next two sections, we will discuss how the force decomposition can be obtained when the force is determined from QM models, including the algebraic description (2) and the dynamics model (7).

3. Force decomposition and local stress in TB models

3.1. TB methods

TB methods represent an important class of approximations that are constructed using basis functions centered around atoms, here denoted by $\phi_\alpha(\boldsymbol{r} - R)$. We also choose $\alpha \in \mathrm{occ}(R_I)$ with $\mathrm{occ}(R_I)$ indicating the set of local orbitals. The wave function ψ_ℓ will be approximated by a linear combinations of atomic orbital.

$$\psi_\ell \approx \sum_I \sum_{\alpha \in \mathrm{occ}(R_I)} c_{\ell,I\alpha}\phi_\alpha(\cdot,R_I), \quad \forall\ \ell = 1, 2, \cdots, N_{\mathrm{ele}}, \tag{15}$$

with coefficients $c_{\ell,I\alpha}$ labeled by the atom I and the local orbital α,

The first step in implementing TB is assembling the overlap and Hamiltonian matrices, defined as follows

$$\begin{aligned} S_{I\alpha,J\beta} &= \langle \phi_\alpha(\cdot,R_I)|\phi_\beta(\cdot,R_J)\rangle, \\ H_{I\alpha,J\beta} &= \langle \phi_\alpha(\cdot,R_I)|\hat{H}|\phi_\beta(\cdot,R_J)\rangle. \end{aligned} \tag{16}$$

The matrix elements only depend on the relative position of the atoms; $R_{IJ} = R_I - R_J$. Namely, we can write $S_{I\alpha,J\beta} \coloneqq M_{\alpha,\beta}(R_{IJ})$. It satisfies the symmetry condition

$$M_{\alpha,\beta}(R_{IJ}) = M_{\beta,\alpha}(R_{JI}). \tag{17}$$

In practice, they are precomputed and represented in parametric forms.

For BOMD, the next step is usually the eigenvalue problem. Using a projection into the subspace spanned by the local orbitals (15), one can reduce the eigenvalue problem (2) into a finite-dimensional generalized eigenvalue problem

$$H\boldsymbol{c}_\ell = \varepsilon_\ell S\boldsymbol{c}_\ell. \tag{18}$$

Here $\boldsymbol{c}_\ell$ is an eigenvector, with elements denoted by $c_{\ell,\ I\alpha}$ as in (15).

Let C be the matrix that contains the eigenvectors as columns. Then the diagonalization can be written simply as

$$HC = SC\Lambda. \tag{19}$$

The diagonal matrix Λ contains the eigenvalues ε_ℓ's.

3.2. The force decomposition

In order to define the force on an ion, we first observe that the total energy, $E_{\mathrm{tot}} = \sum_\ell \varepsilon_\ell n_\ell$, can be written in terms of the Hamiltonian matrix and the eigenvectors

$$E_{\mathrm{tot}} = \sum_\ell \sum_{I\alpha} \sum_{j\beta} H_{I\alpha,J\beta}c_{\ell,I\alpha}c_{\ell,J\beta}n_\ell. \tag{20}$$

By taking the derivative with respect to the ion position R_I, and using the orthogonality condition in (19), one can derive the Hellmann–Feymann formula, which in this case, is given

by

$$\boldsymbol{f}_I = -2\sum_{J\neq I}\sum_{\alpha\in \mathrm{occ}(R_I)}\sum_{\beta\in \mathrm{occ}R_J}\frac{\partial}{\partial R_I}H_{I\alpha,J\beta}n_\ell c_{\ell,I\alpha}c^*_{\ell,J\beta} - 2\sum_{J\neq I}\sum_{\alpha\in \mathrm{occ}(R_I)}\sum_{\beta\in \mathrm{occ}R_J}\frac{\partial}{\partial R_I}S_{I\alpha,J\beta}n_\ell \varepsilon_\ell c_{\ell,I\alpha}c^*_{\ell,J\beta}. \tag{21}$$

The derivative of the eigenvectors with respect to the ion positions does not appear due to the orthogonality conditions (19), but not because they are independent of them.

This provides a natural decomposition

$$\boldsymbol{f}_{IJ} = -2\sum_{\alpha\in \mathrm{occ}(R_I)}\sum_{\beta\in \mathrm{occ}R_J}\frac{\partial}{\partial R_I}H_{I\alpha,J\beta}n_\ell c_{\ell,I\alpha}c^*_{\ell,J\beta} - 2\sum_{\alpha\in \mathrm{occ}(R_I)}\sum_{\beta\in \mathrm{occ}R_J}\frac{\partial}{\partial R_I}S_{I\alpha,J\beta}n_\ell \varepsilon_\ell c_{\ell,I\alpha}c^*_{\ell,J\beta}. \tag{22}$$

This is exactly how the forces are evaluated in the DFTB+ code [5]. The formulas can be simplified, by introducing the density-matrix ρ, and the energy density-matrix Γ, as follows

$$\rho_{I,J} = \sum_{\alpha\in \mathrm{occ}(R_I)}\sum_{\beta\in \mathrm{occ}R_J} n_\ell c_{\ell,I\alpha}c^*_{\ell,J\beta},$$
$$\Gamma_{I,J} = \sum_{\alpha\in \mathrm{occ}(R_I)}\sum_{\beta\in \mathrm{occ}R_J} n_\ell \varepsilon_\ell c_{\ell,I\alpha}c^*_{\ell,J\beta}. \tag{23}$$

Then the force can be written as

$$\boldsymbol{f}_{IJ} = -2\mathrm{tr}\left(\rho_{I,J}\frac{\partial}{\partial R_I}H_{I,J}\right) - 2\mathrm{tr}\left(\Gamma_{I,J}\frac{\partial}{\partial R_I}M_{I,J}\right). \tag{24}$$

The fact that $\boldsymbol{f}_{IJ}$ is skew-symmetric is also evident.

3.3. A numerical test

To verify the desired property of the force decomposition, we consider a silicon nanowire with 512 atoms. The dimension of this quasi one-dimensional system is 96.96 Å × 10.87 Å × 10.87 Å. The nanowire is divided into 16 blocks along the longitudinal direction. By integrating the conservation law (10) in a block, we have

$$\partial_t \boldsymbol{j}_k + \boldsymbol{\tau}_{k+1/2} - \boldsymbol{\tau}_{k-1/2} = 0. \tag{25}$$

Here $\boldsymbol{j}_k$ is the total momentum in the kth block. $\boldsymbol{\tau}$ is the projection of the stress in the longitudinal direction, i.e. $\boldsymbol{\tau} = \sigma \cdot (1, 0, 0)$, and it represents the traction between two adjacent blocks.

We follow the atomic units used in the software package, and modified the code to generate the force components $\boldsymbol{f}_{IJ}$. We ran a BOMD simulation in DFTB+ for 100 steps with step size $\Delta t = 2.067$ (0.05 fs). The initial velocity is randomly chosen. Figure 1 shows the total momentum in a block in the longitudinal direction $j^{(1)}$, and a traverse direction $j^{(2)}(t)$. To examine the calculation of $\boldsymbol{f}_{IJ}$, we computed the traction $\boldsymbol{\tau}$ from the AIMD simulation, and then using the balance equation (25), we reconstructed the velocity at the same time steps. Excellent agreement has been found.

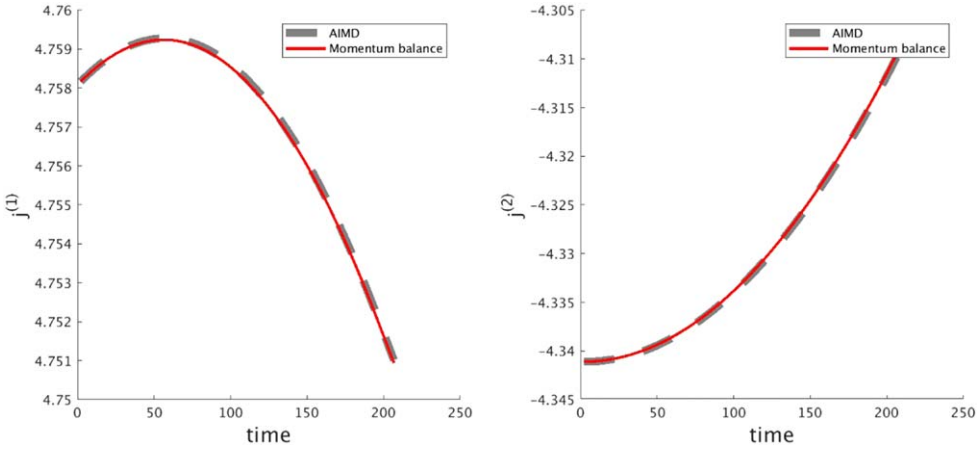

Figure 1. Comparison of the total momentum in a block of a nanowire, one computed from a BOMD simulation in DFTB+ (dashed curve), and the other computed from the momentum balance (25) (solid line).

4. Stress calculation in real-space methods

In real-space methods, the Hamiltonian operator will be discretized using finite difference [51] or finite element methods [52]. The Hamiltonian operator is then represented at the grid points as a matrix, here denoted by H. The numerical procedure in the quantum mechanical model would involve either solving the eigenvalue problem (2) or the TDSEs (7). The main difficulty is that the electronic degrees of freedom are defined at grid points, and they are not specifically tied to the position of the ions.

4.1. Force decomposition and stress calculations

After the eigenvalues are computed from (2), the total energy can be expressed as

$$E_{\text{tot}}(R_1, R_2, \cdots, R_N) = \sum_{\ell} n_\ell \varepsilon_\ell, \tag{26}$$

with n_ℓ's again being the occupation numbers.

The Hellmann–Feymann formula states that the change of the total energy with respect to the change of any parameter λ is given by [53, 54]

$$\frac{\partial}{\partial \lambda} E_{\text{tot}} = \sum_{\ell} n_\ell \langle \psi_\ell | \frac{\partial \hat{H}}{\partial \lambda} | \psi_\ell \rangle. \tag{27}$$

In real-space methods, the Hamiltonian operator is approximated at grid points. The only part of the Hamiltonian that explicitly depends on the ion position is the external potential

$$V_{\text{ext}}(\boldsymbol{r}) = \sum_I \int w(\boldsymbol{r} - R_I) n(\boldsymbol{r}, t)\,\mathrm{d}\boldsymbol{r} + \sum_I \sum_\ell \int\int \psi_\ell(\boldsymbol{r}, t)^* U(\boldsymbol{r} - R_I, \boldsymbol{r}' - R_I)\psi_\ell(\boldsymbol{r}', t)\,\mathrm{d}\boldsymbol{r}\mathrm{d}\boldsymbol{r}' + \frac{1}{2}\sum_{I=1}^{N}\sum_{J\neq I}\frac{Z_I Z_J}{|R_I - R_J|}. \tag{28}$$

Here $n(\boldsymbol{r}, t)$ is the electron density, given by

$$n(\boldsymbol{r}, t) = \sum_{\ell=1}^{N_{\text{ele}}} n_\ell |\psi_\ell(\boldsymbol{r}, t)|^2. \tag{29}$$

Remark. It is worthwhile to point out that in principle, for ground-state calculations, the electron density has an implicit dependence on the ion position. However, the Hellmann–Feymann theorem asserts that the derivatives only need to be taken with respect to the R_I in the external potential.

We will denote the three terms on the right-hand side of (28) as V^{loc}, V^{nloc}, and $V^{\text{i-i}}$, respectively. The term $V^{\text{i-i}}$ is a classical Coulomb interaction and the corresponding force decomposition is trivial, since it has a classical pairwise form and no explicit involvement of the wave functions:

$$\boldsymbol{f}_{IJ}^{\text{i-i}} = \frac{Z_I Z_J (R_I - R_J)}{|R_I - R_J|^3}. \tag{30}$$

Meanwhile, the first two terms stem from the pseudopotential approximation, e.g. norm-preserving potentials [55], which represents the influence of inner-shell electrons and reduce the problem to valence electrons. It represents the ion–electron interactions via a local term, here denoted by $w(\boldsymbol{r})$, which usually only depends on the distance from an ion, and a non-local term, which consists of projections to local orbitals. In practice, this offers considerable reduction in the computational cost. Here we have represented the summation of the projectors by the function U. Interested readers are referred to [55] for specific forms of these terms The details of the force calculations in this case has been explained in the monograph [56].

It suffices to consider the derivatives of the first two terms with respect to the ion positions. Based on the Hellmann–Feymann theorem, we define

$$\begin{aligned}\boldsymbol{f}_I^{\text{loc}} &= \int \nabla w(\boldsymbol{r} - R_I) n(\boldsymbol{r})\,\mathrm{d}\boldsymbol{r},\\ \boldsymbol{f}_I^{\text{nloc}} &= \int\int \psi_\ell(\boldsymbol{r}, t)^* \left(\frac{\partial}{\partial \boldsymbol{r}} + \frac{\partial}{\partial \boldsymbol{r}'}\right) U(\boldsymbol{r} - R_I, \boldsymbol{r}' - R_I)\psi_\ell(\boldsymbol{r}', t)\,\mathrm{d}\boldsymbol{r}\mathrm{d}\boldsymbol{r}'.\end{aligned} \tag{31}$$

In principle, the wave functions ψ_ℓ obtained from DFT or TDDFT model depend on both the electronic coordinates and the atom positions. What makes the Hellmann–Feymann formula (31) appealing is the fact that only the part of the Hamiltonian that depends on the atom position would appear. In particular, the kinetic energy is not involved in (31), and neither is the derivatives of the wave function with respect to the atom positions.

However, this formula does not reveal the interactions among the neighboring atoms, i.e. the decomposition $\boldsymbol{f}_{IJ}$. It is tempting to separate the integrals by dividing the entire domain into non-intersecting subdomains, each of which contains an ion. Our numerical tests suggest that the symmetry condition is not fulfilled. More importantly, in the non-local term, the projectors in U only depend on points close to the atom R_I. As a result, separating the integral would not yield a term that explicitly depends on a neighboring atom R_J. In fact, when the

second formula in (31) is implemented, the force becomes an on-site force, for which a force decomposition is not possible due to (11).

This difficulty has prompted us to rewrite the formula (31) that determines the force and derive alternative expressions. We notice that the wave functions depend on the ion position as well, due to the external potential. Such dependence is implicit in the Feymann–Heymann theorem, since it is canceled when the equation is left-multiplied by an eigen-function, due to the orthogonality. To gain more insight, we observe the explicit dependence of the external potential on the relative positions to the atoms, $\{\boldsymbol{r} - R_I, I = 1, 2, \cdots,\}$, and we will write the wave function as follows

$$\psi_\ell(\boldsymbol{r}, t) = \phi_\ell(\boldsymbol{r} - R_1, \boldsymbol{r} - R_2, \cdots, \boldsymbol{r} - R_{N_{\text{ion}}}, t). \tag{32}$$

Similarly we write the electron density as

$$n(\boldsymbol{r}, t) = d(\boldsymbol{r} - R_1, \boldsymbol{r} - R_2, \cdots, \boldsymbol{r} - R_{N_{\text{ion}}}, t). \tag{33}$$

It is, however, not necessary to know the explicit forms of the functions ϕ_ℓ and d. They are introduced here only to show explicitly the dependence on the ion positions. Now, we turn to the local force (31). Using integration by parts, we obtain

$$\begin{aligned} \boldsymbol{f}_I^{\text{loc}} &= \int \nabla w(\boldsymbol{r} - R_I) n(\boldsymbol{r}, t) \mathrm{d}\boldsymbol{r}, = -\int w(\boldsymbol{r} - R_I) \nabla n(\boldsymbol{r}, t) \mathrm{d}\boldsymbol{r} \\ &= \sum_J \int w(\boldsymbol{r} - R_I) \frac{\partial}{\partial R_J} n(\boldsymbol{r}, t) \mathrm{d}\boldsymbol{r}. \end{aligned} \tag{34}$$

The last step is due to the form (32) and (33). This motivates us to define the force decomposition as follows

$$\boldsymbol{f}_{IJ}^{\text{loc}} = \int w(\boldsymbol{r} - R_I) \frac{\partial}{\partial R_J} n(\boldsymbol{r}, t) \mathrm{d}\boldsymbol{r}. \tag{35}$$

Similarly, we can define the force decomposition for the non-local part

$$\boldsymbol{f}_{IJ}^{\text{nloc}} = 2\,\text{Re} \int\int \psi_\ell(\boldsymbol{r}, t)^* U(\boldsymbol{r} - R_I, \boldsymbol{r}' - R_I) \frac{\partial}{\partial R_J} \psi_\ell(\boldsymbol{r}', t) \mathrm{d}\boldsymbol{r} \mathrm{d}\boldsymbol{r}'. \tag{36}$$

The remaining issue is to determine the change of the wave functions with respect to the change of atom positions, i.e. $\frac{\partial}{\partial R_J}\psi_\ell$. This is done by using the density-functional perturbation theory approach [53]. Let us denote the change of the wave functions, due to an instantaneous change of the position of an ion in one direction, by $\delta\psi$. For the eigenvalue problem (2) that needs to be solved in BOMD, the perturbation yields

$$\begin{aligned} &(\hat{H} - \varepsilon_\ell)\delta\psi_\ell + \int \frac{\delta \hat{V}_{\text{KS}}[n_0(\boldsymbol{r})]}{\delta n(\boldsymbol{r}')} \delta n(\boldsymbol{r}') \mathrm{d}\boldsymbol{r}' \psi_\ell + (\delta \hat{V}_{\text{ext}} - \varepsilon_\ell)\psi_\ell = 0, \\ &\int \psi_\ell^*(\boldsymbol{r}) \delta\psi_\ell(\boldsymbol{r}) + \psi_\ell(\boldsymbol{r}) \delta\psi_\ell^*(\boldsymbol{r}) \mathrm{d}\boldsymbol{r} = 0, \end{aligned} \tag{37}$$

for $\ell = 1, 2, \cdots, N_{\text{ele}}$. Here $n_0(\boldsymbol{r})$ is the ground state electron density, and

$$\delta n(\boldsymbol{r}) = 2\,\text{Re} \sum_\ell n_\ell \psi_\ell^* \delta\psi_\ell$$

will correspond to the term $\frac{\partial}{\partial R_J} n(\boldsymbol{r}, t)$ in (35). $\hat{V}_{\text{KS}}$ is the part of the Hamiltonian that depends on the electron density (4). The term $\delta\hat{V}_{\text{ext}}$ refers to the derivative of the external potential with respect to the ionic position. The second condition in (37) is to ensure the orthogonality of the wave functions.

The equations form a linear system for the wave functions, known as the Sternheimer equation, which can be solved via iterative methods. The coefficients of the linear system only depend on the ground states. So one does not need to solve the eigenvalue problem again. Such an approach has been an important route to determine phonon spectrum, polarizability, dielectric constants, etc [57].

At this point, it is clear that the formulas (35) and (36) would satisfy the property (11). But the skew-symmetric property (12) does not seem to be a direct consequence of our derivation. Here we offer a heuristic argument: suppose that one of the ions, R_J, undergoes an infinitesimally small displacement. In the Sternheimer equation (37), $\hat{V}_{\text{ext}}$ would be a function of $\boldsymbol{r} - R_J$. As a result, we may assume that the perturbed electron density will also be centered around R_J. We assume that it is asymmetric with respect to $\boldsymbol{r} - R_J$, e.g. $\delta n(R_J - \boldsymbol{r}) = -\delta n(\boldsymbol{r} - R_J)$. Therefore, we can write (35) as

$$\boldsymbol{f}_{IJ}^{\text{loc}} = \int w(\boldsymbol{r} - R_I)\delta n(\boldsymbol{r} - R_J)\mathrm{d}\boldsymbol{r}.$$

The local potential w only depends on the relative distance. So by changing variables, $\boldsymbol{r} - R_I = R_J - \boldsymbol{r}'$, we find that

$$\boldsymbol{f}_{IJ}^{\text{loc}} = \int w(\boldsymbol{r} - R_I)\delta n(R_J - \boldsymbol{r})\mathrm{d}\boldsymbol{r} = -\boldsymbol{f}_{JI}^{\text{loc}}.$$

The same argument can be made toward the non-local part of the pseudopotential (36) using a similar assumption on the density matrix.

For Ehrenfest dynamics models, one can again take the derivative of the wave function with respect to the ion position. This procedure yields

$$\mathrm{i}\partial_t \delta\psi_\ell = (\hat{T} + \hat{V}_{\text{KS}}[n_0])\delta\psi_\ell + \int \frac{\delta V_{\text{KS}}[n_0(\boldsymbol{r})]}{\delta n(\boldsymbol{r}')}\delta n(\boldsymbol{r}')\mathrm{d}\boldsymbol{r}'\psi_\ell + \delta\hat{V}_{\text{ext}}\psi_\ell. \tag{38}$$

In practical implementations, one can solve this linear Schrödinger equation to determine $\delta\psi_\ell$, and implement the formulas (30), (35) and (36).

4.2. Numerical tests

We consider a two-dimensional system—a single layer graphene sheet with 32 atoms. The computation is done by using OCTOPUS [6], a real-space implementation of the ground state and TDDFT. Again, we use the standard atomic units. The length unit is Bohr radius and the energy unit is Hartree. All the results will be given in terms of these two units. For the computation, the grid size in the finite-difference approximation is chosen to be 0.2066, and the simulation domain consists of three-dimensional $90 \times 78 \times 40$ grid with center of the rectangular domain shifted to the origin. The dimension of the computational domain is $18.595 \times 16.116 \times 8.265$ (in Bohr radius). Periodic boundary conditions are applied in the first two space dimensions. We chose the standard pseudo-potential set in OCTOPUS.

To create a non-homogeneous stress, we set the initial displacement in the horizontal direction to a sinusoidal profile

$$u_1(\boldsymbol{x}) = \sin\frac{2\pi x_1}{L}, \tag{39}$$

with L being the width of the rectangular domain. The displacement in the other two directions is zero. The atoms will be displaced according to this field in the first two-dimensions with $\boldsymbol{x}$ being the reference coordinates. We set the velocity to zero, so the stress is only due to the elastic field. We modified the part of the OCTOPUS code that computes the phonon spectrum. But instead of computing the vibration frequencies, we followed the linear

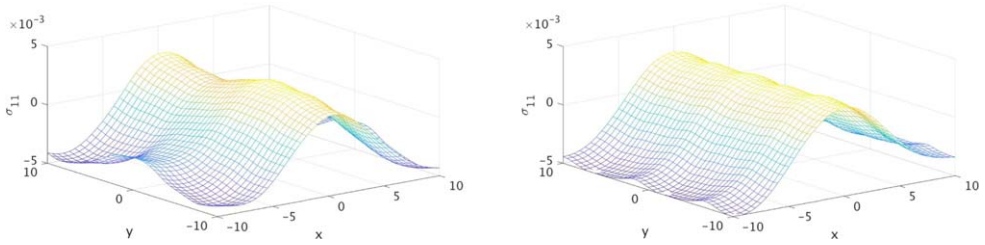

Figure 2. The local stress σ_{11} calculated from the Hardy's formalism using the force decomposition determined from the real-space discretization of the DFT model (left), and the classical MD model with the Tersoff potential.

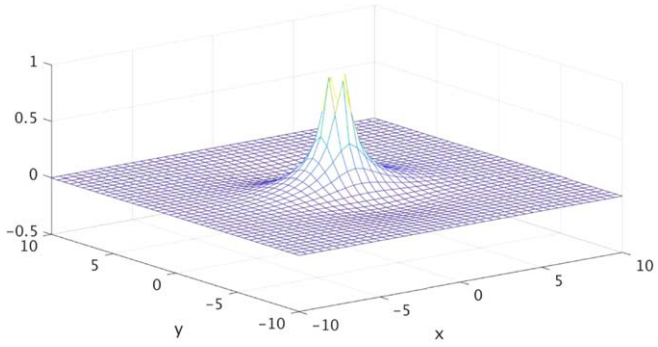

Figure 3. The local strain ϵ_{11} produced by the displacement (41) with $u_{\max} = 0.025$.

response calculations in OCTOPUS and computed $\delta\psi_\ell$. The results are then used to compute the force decomposition in (35) and (36).

With the atoms displaced according to (39), we computed the local Hardy stress using the following two-dimensional kernel function, with a cut-off radius $r_{\text{cut}} = 8$ Bohr

$$\phi(\boldsymbol{x}) = \frac{1}{\pi r_{\text{cut}}^2}\begin{cases} 2\left|\frac{\boldsymbol{x}}{r_{\text{cut}}}\right|^3 - 3\left|\frac{\boldsymbol{x}}{r_{\text{cut}}}\right|^2 + 1, & |\boldsymbol{x}| < r_{\text{cut}} \\ 0, & \text{otherwise.} \end{cases} \tag{40}$$

We compared our results to that from the empirical Tersoff potential, and they exhibit good agreement, as shown in figure 2. In principle, this should not be a means to validate the computational results. But in this particular case, since the displacement is quite smooth, we expect that the two results should be similar.

We now examine the force decomposition property (11). To this end, we consider a less trivial displacement field, as follows

$$\boldsymbol{u}(\boldsymbol{x}) = u_{\max}\, \mathrm{e}^{-0.06|\boldsymbol{x}|^2} \frac{\boldsymbol{x}}{|\boldsymbol{x}|}. \tag{41}$$

The magnitude of the displacement only depends on the distance from the origin. We pick $u_{\max} = 0.5$. The strain field ϵ_{11} is displayed in figure 3. The maximum can be find near the center, with magnitude around 0.8.

Starting with this strain field, we examine the force decomposition property (11), and the results are listed in table 1. To verify the first property (11), we add up $\boldsymbol{f}_{IJ}$ and compare the

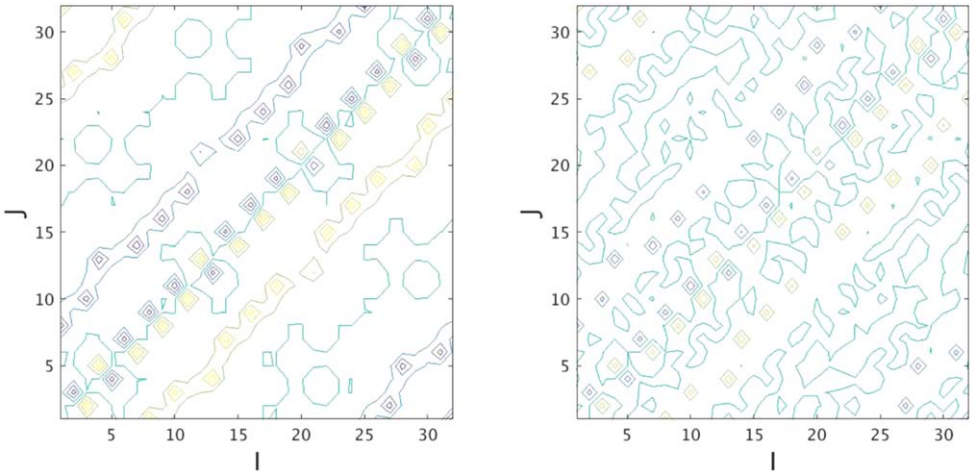

Figure 4. The contour plots of the components of $\boldsymbol{f}_{IJ}$. Left panel: $\boldsymbol{f}_{IJ}^{\mathrm{loc}}$ from (35); right: $\boldsymbol{f}_{IJ}^{\mathrm{nloc}}$ from (36).

Table 1. This table shows the results in the verification of the properties (11) and (12).

Force contributions	$\boldsymbol{f}^{\mathrm{loc}}$	$\boldsymbol{f}^{\mathrm{nloc}}$	$\boldsymbol{f}^{\mathrm{i-i}}$
$\frac{\sqrt{\sum_I \lvert \sum_J \boldsymbol{f}_{IJ} - \boldsymbol{f}_I \rvert^2}}{\sqrt{\sum_I \boldsymbol{f}_I^2}}$	0.0040	0.0043	1.2380×10^{-9}
$\frac{\sqrt{\sum_{I,J} \lvert \boldsymbol{f}_{IJ} + \boldsymbol{f}_{JI} \rvert^2}}{\sqrt{\sum_{I,J} \lvert \boldsymbol{f}_{IJ} \rvert^2}}$	0.0284	0.0734	5.1974×10^{-23}

sum with $\boldsymbol{f}_I$, for each of the three contributions, (30), (35) and (36). In the second row, we verify the second property, i.e. the skew-symmetry (12). This is done for each contribution: Local, non-local, and ionic parts. More specifically, we compute the Frobenius norm of the matrix $\boldsymbol{f}_{IJ} + \boldsymbol{f}_{JI}$. Even though the system has non-homogeneous deformation, one can see that the two properties (11) and (12) are satisfied up to some small error. The error from the first row is clearly numerical error, since from the derivations of (35) and (36), the condition (11) should hold exactly. One may also choose to maintain the skew-symmetric property (12) exactly by defining $\tilde{\boldsymbol{f}}_{IJ} = (\boldsymbol{f}_{IJ} - \boldsymbol{f}_{JI})/2$. In this case, the first condition (30) will hold approximately. Figure 4 displays contour plots of the elements of the matrices $\boldsymbol{f}_{IJ}^{\mathrm{loc}}$ and $\boldsymbol{f}_{IJ}^{\mathrm{nloc}}$ to provide a more direct view of the skew-symmetric structure.

Finally, we check the third property. More specifically, we show in figure 5 how the magnitude of the force components $\boldsymbol{f}_{IJ}$ changes with respect to the distance between the two atoms ($r_{IJ} = |R_{IJ}|$). Interestingly, $\boldsymbol{f}_{IJ}$ exhibits a clear decay pattern, but it only becomes significantly smaller beyond the fifth closest neighbors, and negligible when the distance is around 10 Bohr (7th nearest neighbors). This is a lot larger than the cut-off radius of the Tersoff potential [58], also shown in the same figure (The force decomposition for the Tersoff potential can be found in [33]). In fact, there have been observations that the phonon spectrum of graphene will not be captured accurately, unless fifth neighbors are included in the first-principle calculation [59], which seems to coincide with our current observation.

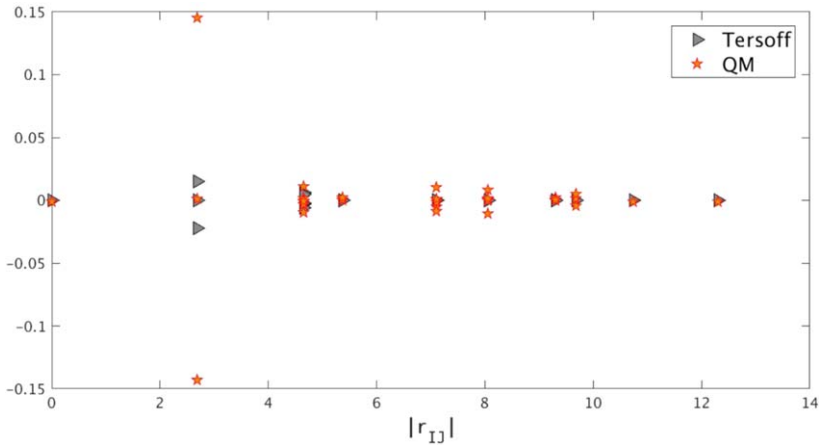

Figure 5. The decay of the force components f_{IJ} and a function of the distance r_{IJ} from the quantum-mechanical (QM) calculation. Also shown is f_{IJ} from the Tersoff potential.

5. Summary and discussions

We have investigated in this paper the appropriate force decomposition in AIMD models. The goal is to be able to define the local stress that can either be used to analyze the elastic field, or be integrated to a continuum description to build a multiscale method. For TB models, it turns out that such decomposition is rather straightforward, due to the fact that the basis functions are centered around the nuclei. For real-space methods, however, this becomes a non-trivial task. We argued that one must estimate the change in the wave functions with respect to the ion displacement in order to obtain such a force decomposition. This perturbation can be computed within the linear response framework by solving the Sternheimer equation.

Acknowledgments

This research was supported by NSF under grant DMS-1522617 and DMS-1819011. We would also like to thank the developers of DFTB+ [5] and OCTOPUS [60] to make the software packages available to our group.

ORCID iDs

Xiantao Li https://orcid.org/0000-0002-9760-7292

References

[1] Marx D and Hutter J 2009 *Ab initio Molecular Dynamics: Basic Theory and Advanced Methods* (Cambridge: Cambridge University Press)
[2] Marx D and Parrinello M 1996 *J. Chem. Phys.* **104** 4077–82
[3] Car R and Parrinello M 1985 *Phys. Rev. Lett.* **55** 2471
[4] Tuckerman M E 2002 *J. Phys:. Condens. Matter* **14** R1297
[5] Aradi B, Hourahine B and Frauenheim T 2007 *J. Phys. Chem.* A **111** 5678–84

[6] Marques M A, Castro A, Bertsch G F and Rubio A 2003 *Comput. Phys. Commun.* **151** 60–78
[7] Giannozzi P *et al* 2009 *J. Phys.: Condens. Matter* **21** 395502
[8] Nielsen O and Martin R M 1983 *Phys. Rev. Lett.* **50** 697
[9] Nielsen O and Martin R M 1985 *Phys. Rev.* B **32** 3792
[10] Filippetti A and Fiorentini V 2000 *Phys. Rev.* B **61** 8433
[11] Shiihara Y, Kohyama M and Ishibashi S 2010 *Phys. Rev.* B **81** 075441
[12] Shiihara Y, Kohyama M and Ishibashi S 2013 *Phys. Rev.* B **87** 125430
[13] Vitek V and Egami T 1987 *Physica Status Solidi* b **144** 145–56
[14] Rogers C L and Rappe A M 2002 *Phys. Rev.* B **65** 224117
[15] Irving J H and Kirkwood J G 1950 *J. Chem. Phys.* **18** 817–29
[16] Hardy R J 1982 *J. Chem. Phys.* **76** 622–8
[17] Hardy R J, Root S and Swanson D R 2002 *AIP Conf. Proc.* **620** 363–6
[18] Admal N C and Tadmor E B 2010 *J. Elast.* **100** 63–143
[19] Andia P, Costanzo F and Gray G 2006 *Modelling Simul. Mater. Sci. Eng.* **14** 741
[20] Andia P, Costanzo F and Gray G 2005 *Int. J. Solids Struct.* **42** 6409–32
[21] Chen Y and Lee J D 2003 *Physica* A **322** 359–76
[22] Chen Y and Lee J D 2003 *Physica* A **322** 377–92
[23] Cormier J, Rickman J M and Delph T J 2001 *J. Appl. Phys.* **89** 99–104
[24] Costanzo F, Gray G L and Andia P C 2005 *Int. J. Eng. Sci.* **43** 533–55
[25] Costanzo F, Gray G L and Andia P C 2004 *Modelling Simul. Mater. Sci. Eng.* **12** S333
[26] Fu Y and To A C 2013 *Modelling Simul. Mater. Sci. Eng.* **21** 055015
[27] Fu Y and To A C 2013 *J. Appl. Phys.* **113** 233505
[28] Lutsko J F 1988 *J. Appl. Phys.* **64** 1152–4
[29] Murdoch A I and Bedeaux D 1994 *Proc. R. Soc.* A **445** 157–79
[30] Murdoch A I and Bedeaux D 1993 *Int. J. Eng. Sci.* **31** 1345–73
[31] Swenson R J 1983 *Am. J. Phys.* **51** 940–2
[32] Tsai D H 1979 *J. Chem. Phys.* **70** 1375–82
[33] Wu X and Li X 2015 *Modelling Simul. Mater. Sci. Eng.* **23** 015003
[34] Wu X, Yang J Z and Li X 2012 *J. Chem. Phys.* **137** 134104
[35] Yang J Z, Wu X and Li X 2012 *J. Chem. Phys.* **137** 134104
[36] Zhou M 2003 *Proc. R. Soc.* A **459** 2347–92
[37] Zhou M and McDowell D L 2002 *Phil. Mag.* A **82** 2547–74
[38] Zimmerman J A, Jones R E and Templeton J A 2010 *J. Comput. Phys.* **229** 2364–89
[39] Zimmerman J A, Webb E B III, Hoyt J J, Jones R E, Klein P A and Bammann D J 2004 *Modelling Simul. Mater. Sci. Eng.* **12** S319
[40] Nielsen O and Martin R M 1985 *Phys. Rev.* B **32** 3780
[41] Kohn W and Sham L J 1965 *Phys. Rev.* **140** A1133
[42] Gross E and Kohn W 1990 Time-dependent density-functional theory *Advances in Quantum Chemistry* vol 21 (Amsterdam: Elsevier) pp 255–91
[43] Ullrich C A 2011 *Time-Dependent Density-Functional Theory: Concepts and Applications* (Oxford: Oxford University Press)
[44] Gruber E *et al* 2016 *Nat. Commun.* **7** 13948
[45] Niklasson A M, Tymczak C and Challacombe M 2006 *Phys. Rev. Lett.* **97** 123001
[46] Alonso J L, Castro A, Clemente-Gallardo J, Cuchí J C, Echenique P and Falceto F 2011 *J. Phys. A: Math. Theor.* **44** 395004
[47] Kühne T D, Krack M, Mohamed F R and Parrinello M 2007 *Phys. Rev. Lett.* **98** 066401
[48] Li X, Tully J C, Schlegel H B and Frisch M J 2005 *J. Chem. Phys.* **123** 084106
[49] Lin L, Lu J and Shao S 2013 *Entropy* **16** 110–37
[50] Runge E and Gross E K 1984 *Phys. Rev. Lett.* **52** 997
[51] Beck T L 2000 *Rev. Mod. Phys.* **72** 1041
[52] Motamarri P, Nowak M R, Leiter K, Knap J and Gavini V 2013 *J. Comput. Phys.* **253** 308–43
[53] Baroni S, de Gironcoli S, Corso A D and Giannozzi P 2001 *Rev. Mod. Phys.* **73** 515–62
[54] Gonze X and Lee C 1997 *Phys. Rev.* B **55** 10355–68
[55] Hamann D, Schlüter M and Chiang C 1979 *Phys. Rev. Lett.* **43** 1494
[56] Kikuji H, Tomoya O and Yoshitaka F 2005 *First-principles Calculations in Real-space Formalism: Electronic Configurations and Transport Properties of Nanostructures* (Singapore: World Scientific)

[57] Yabana K, Nakatsukasa T, Iwata J I and Bertsch G 2006 *Physica Status Solidi* b **243** 1121–38
[58] Tersoff J 1986 *Phys. Rev. Lett.* **56** 632–5
[59] Mohr M, Maultzsch J, Dobardžić E, Reich S, Milošević I, Damnjanović M, Bosak A, Krisch M and Thomsen C 2007 *Phys. Rev.* B **76** 035439
[60] Castro A, Appel H, Oliveira M, Rozzi C A, Andrade X, Lorenzen F, Marques M A, Gross E and Rubio A 2006 *Physica Status Solidi* b **243** 2465–88